Rotating NSs/QSs and recent astrophysical observations

To cite this article: Ang Li and Jianmin Dong 2017 *J. Phys.: Conf. Ser.* **861** 012014

View the article online for updates and enhancements.

Rotating NSs/QSs and recent astrophysical observations

Ang Li[1] and Jianmin Dong[2]

[1] Department of Astronomy, Xiamen University, Xiamen, Fujian 361005, China
[2] Institute of Modern Physics, Chinese Academy of Sciences, Lanzhou 730000, China

E-mail: [1]`liang@xmu.edu.cn`

E-mail: [2]`dongjm07@impcas.ac.cn`

Abstract. Both fast and slow configurations of rotating neutron stars (NSs) are studied with the recently-constructed unified NS EoSs. The calculations for pure quark stars (QSs) and hybrid stars (HSs) are also done, using several updated quark matter EoSs and Gibbs construction for obtaining hadron-quark mixed phase. All three types of EoSs fulfill the recent 2-solar-mass constraint. By confronting the glitch observations with the theoretical calculations for the crustal moment of inertia (MoI), we find that the glitch crisis is still present in Vela-like pulsars. An upcoming accurate MoI measurement (eg., a possible 10% accuracy for pulsar PSR J0737-3039A) allows one to distinguish QSs from NSs, since the MoIs of QSs are generally $\gtrsim 1.5$ times larger than NSs and HSs, no matter the compactness and the mass of the stars. Using tabulated EoSs, we compute stationary and equilibrium sequences of rapidly rotating, relativistic stars in general relativity from the well-tested rns code, assuming the matter comprising the star to be a perfect fluid. All three observed properties of the short gamma-ray bursts (SGRBs) internal plateaus sample are simulated using the rotating configurations of NSs/QSs as basic inputs. We finally argue that for some characteristic SGRBs, the post-merger products of NS-NS mergers are probably supramassive QSs rather than NSs, and NS-NS mergers are a plausible location for quark deconfinement and the formation of QSs.

1. Introduction
Neutron stars (NSs) are by far one of the most interesting observational objects, since many mysteries remain on them due to their complexity. Future observations with advanced telescopes such as SKA, Advanced LIGO/VIRGO, AXTAR, FAST, NICER, LOFT, and eXTP, will certainly improve our current knowledge of such stellar objects, by providing precise measurements of their masses, radii, spin frequencies, glitches, surface temperatures, luminosities, magnetic strengthes, etc. Theoretically, since no first-principle theory can be used due to the non-perturbative nature of quantum chromodynamics at finite chemical density, their inner structures are still unclear. There is also the hypothesis of pure quark stars (QSs) and their transitions to NSs are both intriguing and important open problems. Therefore, for the study of NSs/QSs, particular attention should be paid on combining realistic enough theoretical models with accumulated observations. The present contribution is along this line.

For this purpose, we select unified NS EoSs that satisfy up-to-date experimental constraints from both nuclear physics [1] and astrophysics [2, 3, 4], based on modern nuclear many-body theories, including microscopic methods (e.g. BCPM [5]) starting from a realistic nucleon-nucleon

two-body force (usually accompanied with a nucleonic three body force) and phenomenological ones (e.g. BSk20, BSk21 [6], Shen [7]), starting from a nuclear effective force with parameters fitted to finite nuclei experiments and/or nuclear saturation properties; we also find typical parameter sets for QS EoSs in developed confinement density-dependent mass (CDDM) model, labelled as CIDDM, CDDM1, CDDM2 (see [8] and references therein). Hadron-quark mixed phase is obtained by Gibbs construction [9, 10] and the calculations of hybrid stars (HSs) are done in this framework. All three types of EoSs fulfill the recent 2-solar-mass constraint [2, 3, 4]. For simplicity, several exotic phases possible in NSs' cores are not included here, for example, hyperons (see, e.g., [11]), kaon meson condensation (see, e.g., [12]), Delta excitation (see, e.g., [13]). In the following, we introduce briefly the theoretical framework and discussions of our results in Sects. $2-4$, before providing the summary and future perspectives in Sect. 5. More details can be found in Refs. [8, 14, 15] and references therein.

2. Structures of the Vela pulsar and the glitch crisis

The Vela pulsar (PSR B0833-45) is among the most studied pulsars, which are usually regarded as highly-magnetized, rapidly rotating NSs. By far there is an accurate determination of several pulsar properties, such as the distance, the spin period (89.33 milliseconds), and 17 quasi-periodically produced glitches (sudden increases in spin frequency). Those observations will be used here for a detailed study of its global properties and inner structures. In particular, the "glitch crisis" problem (see eg: [16, 17]), relating to the moment of inertia (MoI) of the stellar crust(see eg: [18, 19]), has generated a great debate recently and will be discussed as well.

Assuming the pulsar mass ranging from $1.0M_\odot$ to $2.0M_\odot$, we calculate the detailed structures of this pulsar, namely the central density, the core/crust radii, the core/crustal mass, the core/crustal thickness, the total/crustal MoI. They are collected in Tables $2-4$ of Ref. [14]. We show here the results from BSk20 EoS as an example.

Furthermore, we analyse the "glitch crisis" problem based on the calculated MoI results. In Fig. 1, the fractional MoIs I_c/I are plotted as a function of the stellar mass for three unified NS EoSs (BCPM, BSk20, BSk21), to be compared with one matched EoS "BHF + NV + BPS". We first notice that for the previous glitch constraint $I_c/I \geq 1.6\%$, the mass of the Vela pulsar should only be smaller than $1.8M_\odot$ based on selected NS EoS models here. This could be easily fulfilled for an isolated pulsar. However, the discovered crustal entrainment shifts the constraint to around $I_c/I \geq 7\%$, which could hardly be fulfilled by a pulsar heavier than $1.0M_\odot$, except a narrow range of $1.0 \sim 1.06M_\odot$ in the matched "BHF + NV + BPS" EoS case. Actually the predicted fractional moments of inertia based on three unified NS EoSs (BCPM, BSk21, BSk20) are no more than 6.48%. Therefore, we argue that the crisis could be still present in the standard two-component model.

3. NSs or QSs? MoI as a probe

The coexistence of NSs and QSs has been a great puzzle. Recently, it has been suggested to measure MoI rather accurately for pulsar PSR J0737-3039A, with a 10% accuracy (or a constraint on $R \sim 5\%$), using the double pulsar system within the next 20 years. This would significantly constrain the EoS for dense stellar matter and may serve as a tool to justify/discriminate NSs/QSs, see references [20, 21, 22, 23, 24, 25] and references therein for more details.

In Ref. [9], we developed our previous study [10] of the transition to deconfined quark phase in NSs, by including the interaction in the quark EoS to the leading order in the perturbative expansion within the CDDM model. Using the Gibbs conditions the hadron-quark mixed phase is constructed matching the latter with the hadron EoS derived from the microscopic Brueckner theory. High-mass HSs consistent with 2-solar-mass constraint are possible with mixed-phase core with typical parameter sets. Together with EoS models based on the same theories for pure NSs and QSs, respectively, we are ready to evaluate the MoIs of three types of compact stars,
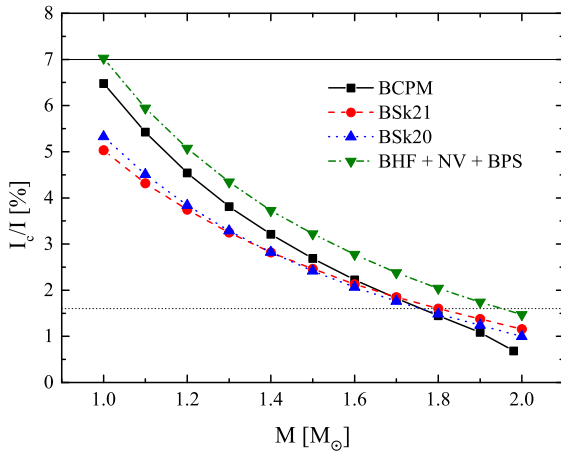
Figure 1. Fractional moments of inertia I_c/I as a function of the stellar mass, with three unified NS EoSs (BCPM, BSk21, BSk20) and one of the matched EoSs (BHF + NV +BPS). Taken from Ref. [14] and see there for details.

Table 1. Predictions for the properties of the Vela pulsar (PSR B0833-45) with a spin period of 89.33 milliseconds, taking the pulsar mass ranging from $1.0 M_\odot$ to $2.0 M_\odot$. The central densities are in units of fm^{-3}, the masses in solar masses $M_\odot$ (except the mass of the outer crust M_{ocrust} in $10^{-5} M_\odot$), the radii in kilometers, the total moments of inertia in $10^{45} g\ cm^2$, and the fractional moments of inertia in percentage. Calculations are done with the BSk20 NS EoS, which is based on the widely-used Skyrme nuclear energy density functional, and the parameters were fitted to reproduce with high accuracy almost all known nuclear masses, and to various physical conditions including the nuclear matter EoS from microscopic calculations. Taken from Ref. [14] and see there for details and more results on other unified EoSs (eg: BCPM, BSk21).

Mass	Cent.	Mass				Radius			Moment of inertia	
		core	icrust	ocrust	total	core	icrust	ocrust	total	fraction
1.0	0.328	0.97	0.025	5.57	12.50	10.93	0.84	0.73	1.001	5.03
1.1	0.346	1.08	0.023	5.08	12.54	11.13	0.76	0.65	1.154	4.32
1.2	0.365	1.18	0.022	4.68	12.58	11.30	0.69	0.58	1.315	3.75
1.3	0.384	1.28	0.021	4.25	12.60	11.44	0.63	0.53	1.482	3.25
1.4	0.405	1.38	0.019	3.93	12.62	11.57	0.57	0.48	1.657	2.82
1.5	0.428	1.48	0.018	3.57	12.62	11.67	0.52	0.43	1.839	2.46
1.6	0.453	1.58	0.016	3.27	12.61	11.74	0.48	0.39	2.026	2.13
1.7	0.480	1.68	0.015	2.93	12.58	11.79	0.43	0.35	2.220	1.85
1.8	0.511	1.79	0.014	2.63	12.52	11.82	0.39	0.31	2.420	1.60
1.9	0.548	1.89	0.012	2.34	12.44	11.81	0.35	0.28	2.624	1.38
2.0	0.593	1.99	0.011	2.05	12.32	11.76	0.31	0.25	2.833	1.16

and study whether or not the upcoming MoI constraint might serve as probe for high-density phase of stellar matter. In addition, previous studies (eg: [20, 21]) found large spread in the results for self-bound QSs. The reason might be relatively free parameters in QS models which determine the surface density of strange quark matter at zero pressure. This situation could be largely improved by the new 2-solar-mass constraint used in the present study.

Fig. 2 presents the stars' gravitational masses as functions of central density for these EoSs models (NSs in solid black line, SSs in solid red and blue lines, and HSs in dash-dotted blue

line), together with two recent massive stars (PSR J1614-2230 [2, 3] and PSR J0348+0432 [4])
whose masses are accurately measured. The horizontal line represents the pulsar mass $1.337M_\odot$
of PSR J0737-3039A. The calculated MoI of QSs are generally $> \sim 1.5$ times larger than those of
NSs and HSs, no matter the compactness and the mass of the stars. This is consistent with the
calculations in Ref. [23]. Fig. 3 shows the scaled MoIs as a function of stellar mass, in comparison
with an upcoming accurate MoI measurement (indicated by a shadowed area like Ref. [22]). One
sees that such measurement could have the ability to distinguish QSs from NSs/HSs. More model
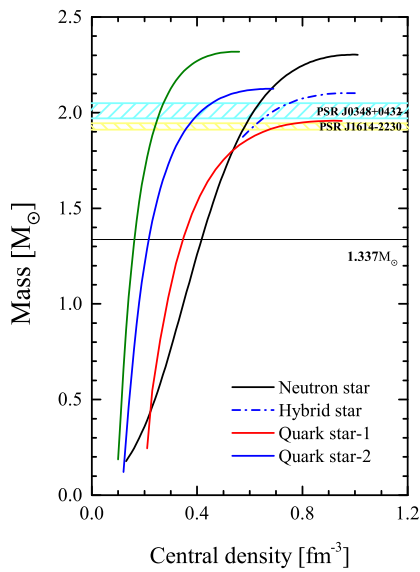calculations should be done to justify this argument as a model-independent one.

Figure 2. Gravitational masses as functions of the stars' central densities for NSs, HSs and QSs, together with two recently-measured massive stars. The horizontal line represents the pulsar mass $1.337M_\odot$ of PSR J0737-3039A. Taken from Ref. [15] and see there for details.
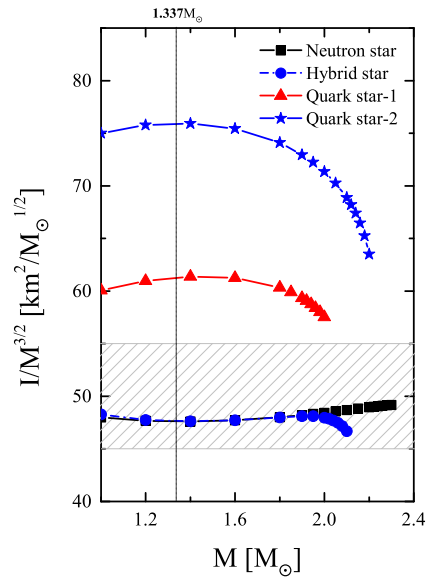
Figure 3. Scaled MoI as a function of stellar mass, based on EoS models in Fig. 2. Shadowed area indicates an upcoming accurate MoI measurement [22]. The vertical line represents the pulsar mass $1.337M_\odot$ of PSR J0737-3039A. Taken from Ref. [15] and see there for details.

4. Internal X-ray plateau in short GRBs: Signature of supramassive fast-rotating QSs?

Short gamma-ray bursts (SGRBs) are generally believed to originate from the mergers of two
NSs or one NS and one black hole (NS-BH). The traditional view is that NS-NS mergers produce
a BH promptly or less than 1 second after the merger, and accretion of remaining debris into
the BH launches a relativistic jet that powers the SGRB. Such an engine is also naturally
expected within NS-BH merger systems. $Swift$ observations of SGRBs, on the other hand,
showed extended central engine activities in the early X-ray afterglow phase, in particular the
so-called internal plateau, characterized by a nearly flat light curve plateau extending to ~ 300
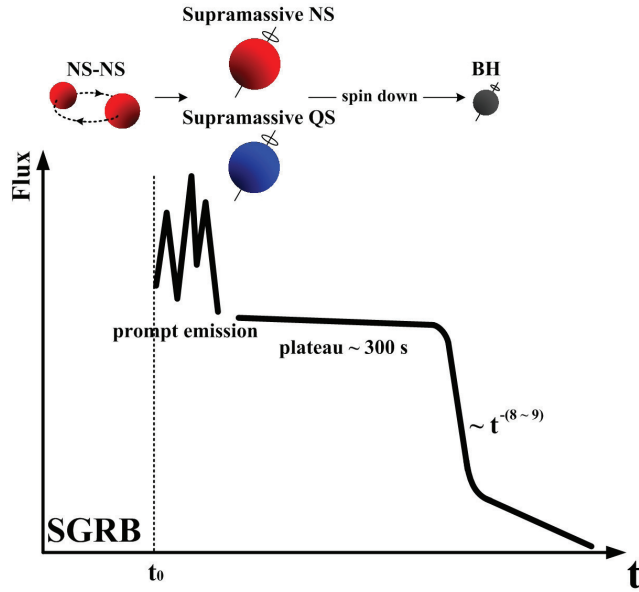seconds followed by a rapid $t^{-(8\sim 9)}$ decay, as shown in Fig. 4.

Figure 4. Illustration of the "internal plateau" observation and the NS/QS central engine model in SGRBs.

Table 2. NS/QS EoSs investigated in this study. Here P_K, $I_{K,max}$ are the Keplerian spin limit and the corresponding maximum moment of inertia, respectively; M_{TOV}, R_{eq} are the static gravitational maximum mass and the corresponding equatorial radius, respectively; α, β are the fitting parameters for M_{max} in Eq. (1); A, B, C are the fitting parameters for $R_{eq,max}$ in Eq. (2); a, q, k are the fitting parameters for I_{max} in Eq. (3). Taken from Ref. [8] and see there for details.

	EoS	P_K (ms)	$I_{K,max}$ (10^{45}g cm^2)	M_{TOV} ($M_\odot$)	R_{eq} (km)	α ($P^{-\beta}$)	β	A (P^{-B})	B	C (km)	a	q (ms)	k (P^{-1})
	BCPM	0.5584	2.857	1.98	9.941	0.03859	-2.651	0.7172	-2.674	9.910	0.4509	0.3877	7.334
NS	BSk20	0.5391	3.503	2.17	10.17	0.03587	-2.675	0.6347	-2.638	10.18	0.4714	0.4062	6.929
	BSk21	0.6021	4.368	2.28	11.08	0.04868	-2.746	0.9429	-2.696	11.03	0.4838	0.3500	7.085
	Shen	0.7143	4.675	2.18	12.40	0.07657	-2.738	1.393	-3.431	12.47	0.4102	0.5725	8.644
	CIDDM	0.8326	8.645	2.09	12.43	0.16146	-4.932	2.583	-5.223	12.75	0.4433	0.8079	80.76
QS	CDDM1	0.9960	11.67	2.21	13.99	0.39154	-4.999	7.920	-5.322	14.32	0.4253	0.9608	57.94
	CDDM2	1.1249	16.34	2.45	15.76	0.74477	-5.175	17.27	-5.479	16.13	0.4205	1.087	55.14

Since it is very difficult for a BH engine to power such a plateau, one attractive interpretation is that NS-NS mergers produce a rapidly-spinning, supramassive NS rather than a BH, with the rapidly decaying phase signifying the epoch when the supramassive NS collapses to a BH after the NS spins down due to dipole radiation or gravitational wave radiation. Whether the current modelling of a NS could reproduce reasonably all three observed quantities (the break time t_b, the break time luminosity L_b and the total energy in the electromagnetic channel E_{total}) is crucially related to the underlying EoS of dense nuclear matter and the calculated rotating configurations.

While a previous analysis shows a qualitative consistency between this suggestion and the *Swift* SGRB data, the distribution of observed break time t_b is much narrower than the distribution of the collapse time of supramassive NSs for the several NS EoSs investigated. We here include developed QS EoSs (labelled as CIDDM, CDDM1, CDDM2), as well as recently-constructed unified NS EoSs (BCPM, BSk20, BSk21, Shen). The corresponding star properties are collected in the first four rows of Table 2. Rotating configurations (M_{max}, R_{eq}, I_{max}) from

Table 3. Simulated parameter ranges for supramassive NS/QS properties from the *Swift* internal plateaux sample with EoS models (BSk20, BSk21, Shen, CIDDM, CDDM1, CDDM2). Here ϵ, P_i, B_p, η are the ellipticity, the initial spin period, the surface dipole magnetic field, and the radiation efficiency, respectively. $P_{\mathrm{best}}(t_b)$ in the last column is the best P value only for the t_b distribution. It is taken from Ref. [8] and see there for details.

EoS	ϵ	P_i (ms)	B_p (G)	η	P_{best} (t_b)
BSk20	0.002	$0.70 - 0.75$	$N(\mu_{\mathrm{Bp}} = 10^{14.8-15.4}, \sigma_{\mathrm{Bp}} \leq 0.2)$	$0.5 - 1$	0.20
BSk21	0.002	$0.60 - 0.80$	$N(\mu_{\mathrm{Bp}} = 10^{14.7-15.1}, \sigma_{\mathrm{Bp}} \leq 0.2)$	$0.7 - 1$	0.29
Shen	$0.002 - 0.003$	$0.70 - 0.90$	$N(\mu_{\mathrm{Bp}} = 10^{14.6-15.0}, \sigma_{\mathrm{Bp}} \leq 0.2)$	$0.5 - 1$	0.41
CIDDM	0.001	$0.95 - 1.05$	$N(\mu_{\mathrm{Bp}} = 10^{14.8-15.4}, \sigma_{\mathrm{Bp}} \leq 0.2)$	$0.5 - 1$	0.44
CDDM1	$0.002 - 0.003$	$1.00 - 1.40$	$N(\mu_{\mathrm{Bp}} = 10^{14.7-15.1}, \sigma_{\mathrm{Bp}} \leq 0.3)$	$0.5 - 1$	0.65
CDDM2	$0.004 - 0.007$	$1.10 - 1.70$	$N(\mu_{\mathrm{Bp}} = 10^{14.8-15.3}, \sigma_{\mathrm{Bp}} \leq 0.4)$	$0.5 - 1$	0.84

the *rns* code can be fitted well as a function of the spin period (P) (in millisecond) as follows:

$$\frac{M_{\mathrm{max}}}{M_\odot} = \frac{M_{\mathrm{TOV}}}{M_\odot} \left[1 + \alpha \, \left(\frac{P}{\mathrm{ms}} \right)^\beta \right] ; \tag{1}$$

$$\frac{R_{\mathrm{eq,max}}}{\mathrm{km}} = C + A \, \left(\frac{P}{\mathrm{ms}} \right)^B ; \tag{2}$$

$$\frac{I_{\mathrm{max}}}{10^{45} \mathrm{g \, cm}^2} = \frac{M_{\mathrm{max}}}{M_\odot} \, \left(\frac{R_{\mathrm{eq}}}{\mathrm{km}} \right)^2 \frac{a}{1 + e^{-k \left(\frac{P}{\mathrm{ms}} - q \right)}}, \tag{3}$$

where the parameters $(\alpha, \beta, A, B, C, a, q, k)$ are collected in the last eight columns of Table 2.

Before comparing our results with detailed SGRB observations, it is necessary to first check if the chosen NS/QS EoSs could reproduce the current fraction of supramassive stars, $\sim 22\%$, based on the mass distribution observation of Galactic NS-NS binary systems. The details are in Ref. [8] and the results are shown in Fig. 5. One can see that all except the BCPM NS EoS can reproduce the 22% fraction constraint (with slightly different required P_i). In the following we omit the BCPM EoS. The allowed static gravitational maximum mass M_{TOV} is then in the range of $2.17 M_\odot - 2.45 M_\odot$.

We finally apply our previous Monte Carlo simulations to the new EoSs for both NSs and QSs, trying to simultaneously reproduce all three distributions (t_b, L_b, E_{total}) available from the observational data and revealing the post-merger supramassive stars' physics. The results are shown in Table 3 and Fig. 6.

In Table 3, we list the constrained ranges for the NSs'(QSs') parameters: an ellipticity ϵ as low as 0.002 (0.001), an initial spin period P_i commonly close to the Keplerian limit P_{K}, a surface dipole magnetic field of $B_p \sim 10^{15}$ G [satisfying normal distributions $N(\mu_{\mathrm{Bp}}, \sigma_{\mathrm{Bp}})$], and an efficiency of $\eta = 0.5 - 1$ related to the conversion of the dipole spin-down luminosity to the observed X-ray luminosity. In the last column we show $P_{\mathrm{best}}(t_b)$, the best values only for the t_b distribution. It is clear that the KS test for the t_b distribution is indeed improved. In particular, as one can see from Fig. 6, the t_b distributions in the QS scenarios are more concentrated, which provide a better agreement with the observed ones. Some quantitative differences would exist for other QS model EoSs, but the same conclusions should hold because of the similar QS rotational properties obtained (more pronounced increases of M_{max} with frequency than those with the NS ones: $\sim 40\%$ vs. $18 - 20\%$ in the present calculation). We therefore argue that a supramassive
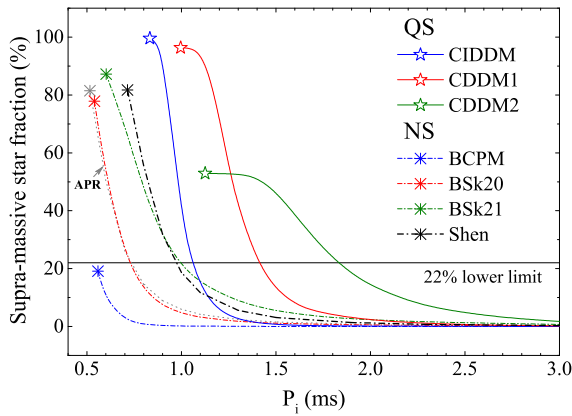
Figure 5. Theoretical estimations of the supramassive star fraction based on four cases of unified NS EoSs and three cases of QS EoSs, as compared with the observed 22% constraint. Previous calculations using the APR NS EoS model [26] are also shown for comparison. Taken from Ref. [8] and see there for details.

QS is favored than a supramassive NS to serve as the central engine of SGRBs with internal plateaux. NS-NS mergers are a plausible location for quark deconfinement and the formation of QSs.
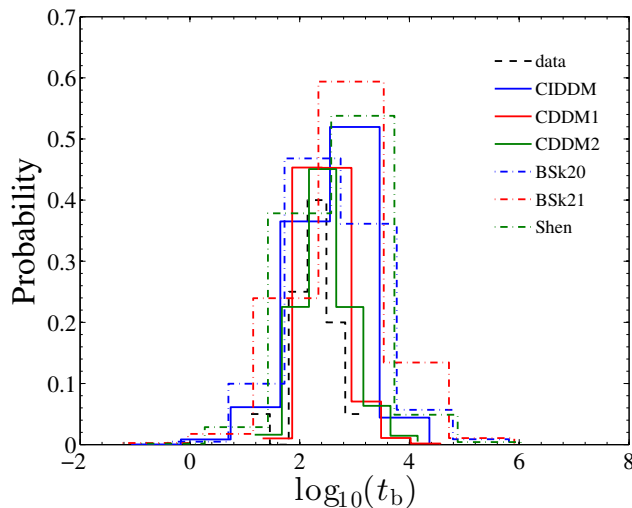

Figure 6. Simulated collapse time distributions with three unified NS EoSs and three QS EoSs, as compared with the observed one (dashed curve). Taken from Ref. [8] and see there for details.

5. Summary and future perspectives

In the present proceeding we show our three recent calculations on rotating compact stars, and compare them with available/upcoming accurate astrophysical observations, including pulsar glitch, MoI, and SQRB.

In terms of future methods, useful constraints could be possible by combining gravitational wave and electromagnetic observations from both coalescing NS-NS binaries and isolated NSs. It would be interesting and meaningful to study whether NS EoS could be determined from gravitational wave emission from elliptically deformed pulsars and NS-NS binaries.

References

[1] Danielewicz P, Lacey R and Lynch W G 2002 *Science* **298**, 1592
[2] Demorest P B, Pennucci R, Ransom S M, Roberts M S E and Hessels J W T 2010 *Nature* **467** 1081
[3] Antoniadis J, et al. 2013 *Science* **340** 6131
[4] Fonseca E *et al* arXiv:1603.00545
[5] Sharma B K, Centelles M, Vinas X, Baldo M and Burgio G F 2015 *Astron. Astrophys* **584** A103
[6] Potekhin A Y, Fantina A F, Chamel N, Pearson J M and Goriely S 2013 *Astron. Astrophys* **560** A48
[7] Shen H, Toki H, Oyamatsu K and Sumiyoshi K 1998 *Nucl. Phys. A* **637** 435
[8] Li A, Zhang B, Zhang N B, Gao H, Qi B and Liu T 2016 *Phys. Rev. D* **94** 083010
[9] Li A, Zuo W and Peng G X 2015 *Phys. Rev. C* **91** 035803
[10] Peng G X, Li A and Lombardo, U. 2008 *Phys. Rev. C* **77** 065807
[11] Hu J N, Li A, Toki H and Zuo W 2014 *Phys. Rev. C* **89** 025802; Burgio G F, Schulze H-J and Li A 2011 *Phys. Rev. C* **83** 025804
[12] Li A, Zhou X R, Burgio G F and Schulze H J 2010 *Phys. Rev. C* **81** 025806; Li A, Burgio G F, Lombardo U and Zuo W 2006 *Phys. Rev. C* **74** 055801; Zuo W, Li A, Li Z H and Lombardo U 2004 *Phys. Rev. C* **70** 055802
[13] Zhu Z Y, Li A, Hu J N and Sagawa H 2016 *Phys. Rev. C* **94** 045803
[14] Li A, Dong J M, Wang J B and Xu R X 2016 ApJS **223**, 16
[15] Li A and Dong J M, to be submitted
[16] Andersson N, Glampedakis K, Ho W C and Espinoza C M 2012 *Phys. Rev. Lett.* **109** 241103
[17] Chamel N 2013 *Phys. Rev. Lett.* **110** 011101
[18] Link B, Epstein R I and Lattimer J M 1999 *Phys. Rev. Lett.* **83** 3362
[19] Li A 2015 *Chin. Phys. Lett.* **32** 079701
[20] Morrison I A, Baumgarte T W, Shapiro S L and Pandharipande V R 2004 ApJ **617** L135
[21] Bejger M, Bulik T and Haensel P 2005 MNRAS **364**, 635
[22] Lattimer J M and Schutz B F 2005 ApJ **629** 979
[23] Urbanec M, Miller J C and Stuchlik Z 2013 MNRAS **433** 1903
[24] Rikovska S J, Guichon P A M, Matevosyan H H and Thomas A W 2007 *Nucl. Phys. A* **792** 341
[25] Li A, Xu R X and Lu J F 2010 MNRAS **402** 2715; Li A, Peng G X and Lu J F 2011 *Res. Astron. and Astrophys.* **11** 482
[26] Akmal A, Pandharipande V R and Ravenhall D G 1998 *Phys. Rev. C* **58** 1804